Title

Two transmembrane dimers of the bovine papillomavirus E5 oncoprotein clamp the PDGF β receptor in an active dimeric conformation

Journal

Proceedings of the National Academy of Sciences of the United States of America, 114(35)

ISSN

0027-8424

Authors

Karabadzhak, Alexander G
Petti, Lisa M
Barrera, Francisco N
et al.

Publication Date

2017-08-29

DOI

10.1073/pnas.1705622114

Peer reviewed

Two transmembrane dimers of the bovine papillomavirus E5 oncoprotein clamp the PDGF β receptor in an active dimeric conformation

Alexander G. Karabadzhak[a,1], Lisa M. Petti[b,1], Francisco N. Barrera[c], Anne P. B. Edwards[b], Andrés Moya-Rodríguez[b], Yury S. Polikanov[a,2], J. Alfredo Freites[d], Douglas J. Tobias[d], Donald M. Engelman[a,e,3], and Daniel DiMaio[a,b,e,f,3]

[a]Department of Molecular Biophysics & Biochemistry, Yale University, New Haven, CT 06520-8024; [b]Department of Genetics, Yale School of Medicine, New Haven, CT 06520-8005; [c]Department of Biochemistry and Cellular and Molecular Biology, University of Tennessee, Knoxville, TN 37996-0800; [d]Department of Chemistry, University of California, Irvine, CA 92697-2025; [e]Yale Cancer Center, New Haven, CT 06520-8028; and [f]Department of Therapeutic Radiology, Yale School of Medicine, New Haven, CT 06520-8040

Contributed by Donald M. Engelman, July 12, 2017 (sent for review April 6, 2017; reviewed by Paul Lambert, Alessandro Senes, and Steven O. Smith)

The dimeric 44-residue E5 protein of bovine papillomavirus is the smallest known naturally occurring oncoprotein. This transmembrane protein binds to the transmembrane domain (TMD) of the platelet-derived growth factor β receptor (PDGFβR), causing dimerization and activation of the receptor. Here, we use Rosetta membrane modeling and all-atom molecular dynamics simulations in a membrane environment to develop a chemically detailed model of the E5 protein/PDGFβR complex. In this model, an active dimer of the PDGFβR TMD is sandwiched between two dimers of the E5 protein. Biochemical experiments showed that the major PDGFβR TMD complex in mouse cells contains two E5 dimers and that binding the PDGFβR TMD to the E5 protein is necessary and sufficient to recruit both E5 dimers into the complex. These results demonstrate how E5 binding induces receptor dimerization and define a molecular mechanism of receptor activation based on specific interactions between TMDs.

transmembrane protein complex | oncogene | traptamer | BPV | blue native gel electrophoresis

Because viruses modulate signaling nodes that control cell behavior and virus replication, the study of viral proteins has provided great insight into many aspects of cellular biochemistry and the cellular processes that regulate biological function. Thus, viral proteins have long been recognized as valuable tools to probe central problems in biology. A particularly interesting viral protein is the 44-residue E5 oncoprotein encoded by bovine papillomavirus type 1 (BPV). The BPV E5 protein and closely related E5 proteins of other fibropapillomaviruses are the shortest known, naturally occurring proteins with tumorigenic potential (1). The E5 protein is an extremely hydrophobic integral membrane protein located primarily in the membranes of the Golgi apparatus of transformed cells (2, 3). Biophysical studies in model membranes indicate that the E5 protein adopts a transmembrane orientation roughly perpendicular to the membrane surface (4–6). In essence, the E5 protein is a free-standing transmembrane domain (TMD), with a type II transmembrane orientation in which a short C-terminal segment protrudes into the lumen of the Golgi (2). In cells, detergent micelles, and model lipid bilayers, the E5 protein exists as a homodimer stabilized by disulfide bonds involving C-terminal cysteine residues (3–5, 7–10). Genetic studies showed that E5 dimerization is required for transforming activity, and a preferred orientation of the E5 dimer with a symmetric homodimer interface has been identified (7, 9, 11, 12).

The E5 protein transforms cells by activating the cellular platelet-derived growth factor (PDGF) β receptor (PDGFβR), although there may be additional minor, alternative transforming pathways as well (13). The PDGFβR is a receptor tyrosine kinase (RTK) with an extracellular domain that binds PDGF, a hydrophobic membrane-spanning segment, and a cytoplasmic domain with tyrosine kinase activity. The inactive PDGFβR is primarily monomeric in unstimulated cells, and PDGF binding induces receptor dimerization and activation of kinase activity, resulting in receptor autophosphorylation and the initiation of a mitogenic signaling cascade (14, 15).

The E5 protein uses an unusual biochemical mechanism to activate the PDGFβR. Unlike PDGF, which binds to the extracellular domain of the PDGFβR, the E5 protein binds to the TMD of the receptor, thereby causing receptor dimerization (16–20). Genetic studies imply that the E5 protein and the PDGFβR TMDs align side by side in the membrane and contact one another directly, a conclusion supported by biophysical studies with purified E5 and PDGFβR TMD peptides (4, 5, 9, 12, 21–25). Because the E5 protein and the PDGFβR adopt opposite transmembrane orientations (type II for E5 and type I—i.e., N terminus in the luminal space—for the PDGFβR), their TMDs are antiparallel. The E5 protein does not bind or activate other RTKs, not even the closely related PDGF α receptor, implying that highly specific interactions between the E5 protein and the

Significance

Highly specific protein–protein interactions between transmembrane domains play crucial roles in many biological processes, but are difficult to study because they occur within membranes. The E5 protein of bovine papillomavirus is a 44-residue transmembrane protein that transforms cells by binding the transmembrane domain of the PDGF receptor, resulting in receptor activation. By combining computational modeling, genetic analysis, and biochemical studies, we propose a quaternary structure of the complex between the E5 protein and the PDGF receptor, in which two dimers of the E5 protein clamp two molecules of the receptor transmembrane domain into an active dimeric conformation. These studies reveal the molecular mechanism of action of an unusual oncogene and provide a pathway to study biologically interesting transmembrane complexes.

Author contributions: A.G.K., L.M.P., F.N.B., A.P.B.E., Y.S.P., J.A.F., D.J.T., D.M.E., and D.D. designed research; A.G.K., L.M.P., F.N.B., A.P.B.E., A.M.-R., and Y.S.P. performed research; A.G.K., L.M.P., F.N.B., A.P.B.E., J.A.F., D.J.T., D.M.E., and D.D. analyzed data; and A.G.K., L.M.P., F.N.B., Y.S.P., J.A.F., D.J.T., D.M.E., and D.D. wrote the paper.

Reviewers: P.L., University of Wisconsin; A.S., University of Wisconsin; and S.O.S., Stony Brook University.

The authors declare no conflict of interest.

[1]A.G.K. and L.M.P. contributed equally to this work.

[2]Present addresses: Department of Biological Sciences and Department of Medicinal Chemistry and Pharmacognosy, University of Illinois at Chicago, Chicago, IL 60607.

[3]To whom correspondence may be addressed. Email: daniel.dimaio@yale.edu or donald.engelman@yale.edu.

This article contains supporting information online at www.pnas.org/lookup/suppl/doi:10.1073/pnas.1705622114/-/DCSupplemental.

PDGFβR are responsible for activation (26–28). In addition to causing PDGFβR activation, complex formation between the E5 protein and the PDGFβR may help adapt the relatively long TMD of the PDGFβR to the thin lipid bilayer of the Golgi membrane (4, 29).

Mutational analysis of the E5 protein and the PDGFβR TMD identified a number of residues important for complex formation between these two proteins. Complex formation and biological activity are crucially dependent on Gln-17 and Asp-33 of E5 and Lys-499 and Thr-513 in the PDGFβR (12, 18, 21, 23–25, 30, 31). These findings suggested that E5 Asp-33 and PDGFβR Lys-499 form a salt bridge in the juxtamembrane luminal/extracellular domain of the proteins and that E5 Gln-17 hydrogen-bonds to PDGFβR Thr-513 within the membrane itself.

On the basis of these studies and computational analysis, several models of the complex between the E5 protein and the PDGFβR TMD have been proposed (4, 6, 9, 12, 23). In each of these models, the complex consists of a single dimer of the E5 protein bridging two molecules of the PDGFβR TMD, but the stoichiometry of the complex has not been established. Moreover, because of the technical difficulties of studying TMD complexes in membranes, no high-resolution structural information about the complex in the active state has been obtained. Thus, it is not known how E5 binding induces dimerization of the PDGFβR TMDs, the central event in receptor activation.

Here, we used a combination of computational modeling and genetic and biochemical analysis to generate a chemically detailed model for the complex between the E5 protein and the PDGFβR. Rosetta membrane modeling constrained by experimental evidence was used to select an initial structural model, followed by all-atom molecular dynamics (MD) simulations in a hydrated lipid bilayer environment. The results of this modeling suggested that the previous models consisting of one E5 dimer and two PDGFβR TMDs did not correctly assign the stoichiometry of the complex. Rather, an alternative stoichiometry consisting of two E5 dimers in a complex with two PDGFβR TMDs allowed close packing between the PDGFβR TMDs, thus driving receptor dimerization. Biochemical analysis of the complex in cells expressing the E5 protein and various wild-type, mutant, and truncated versions of the PDGFβR provided strong support for this model, which provides chemical insight into the molecular mechanism of how E5 binding induces receptor activation. Better understanding of the interaction of the E5 protein and the PDGFβR TMDs and how it results in receptor activation not only establishes the molecular basis for this extraordinary mechanism of oncogenesis, but also provides important insight into higher-order interactions that can occur between TMDs. Because up to 30% of all eukaryotic proteins contain TMDs, detailed analysis of this important class of interactions will inform our molecular understanding of many cellular processes.

Results

Rosetta Membrane Modeling. We used Rosetta membrane modeling (32) to create a starting coarse-grained model of the E5–PDGFβR complex. Because the Rosetta membrane protocol was developed for multipass transmembrane proteins, we first converted the independent TMDs of the E5 protein and the PDGFβR into a single polypeptide chain in silico. Two BPV E5 proteins and two PDGFβR TMDs were connected in alternating order [N–PR(I)–E5(I)–PR(II)–E5(II)–C] with glycine–glycine mock extramembrane linkers to create a single molecule we refer to as "the snake" (Fig. 1*A*). This alternating arrangement enforced the antiparallel orientation of the E5 and PDGFβR segments as they crossed the membrane.

An overview of the modeling approach is presented in Fig. 1*B*. In the Rosetta membrane protocol, the TMDs were inserted sequentially into the membrane bilayer, and 50,000 Monte Carlo simulations were carried out to identify low-energy structures.

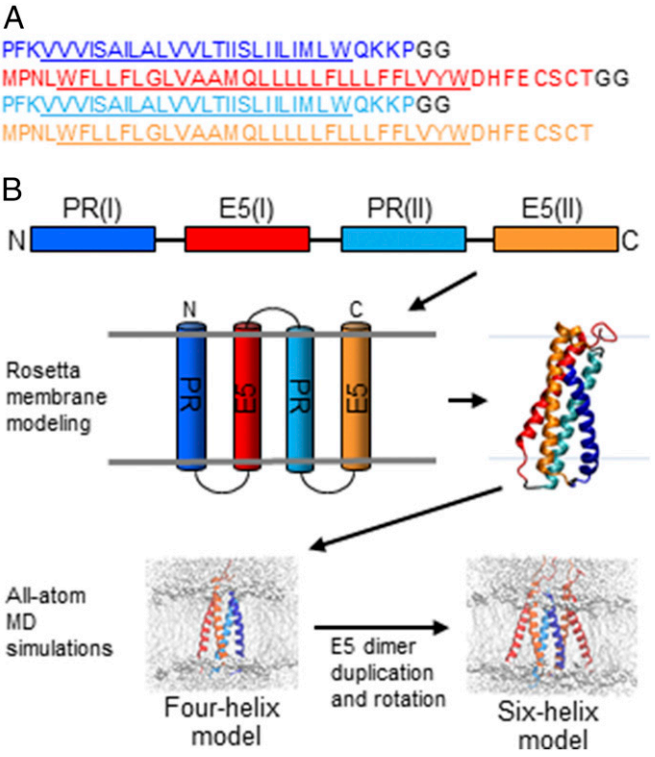

Fig. 1. Modeling strategy. (*A*) Amino acid sequence of the virtual snake consisting of two TMDs of the PDGFβR and two TMDs of the BPV E5 protein. E5 sequences are orange [E5(I)] and red [E5(II)], PDGFβR TMD sequences are dark [PR(I)] and light [PR(II)] blue, and glycine linkers are black, with the predicted TMDs underlined. All sequences are written N-to-C. (*B*) Schematic overview of the multistep modeling strategy. Color scheme is as in *A*.

The 50 clusters of structures with the lowest energies were analyzed further, as described in detail in *Materials and Methods* (Fig. S1). Briefly, to select the most robust Rosetta model, we used several criteria based on prior mutational data and evolutionary considerations to exclude all but one model: (*i*) We excluded clusters that were incompatible with mutational data suggesting the existence of three specific side-chain interactions and a preferred E5 dimer interface. Specifically, a cluster was further considered only if the structure allowed formation of: (*a*) an intermolecular disulfide bond between Cys-37 and/or Cys-39 in different E5 monomers; (*b*) a salt bridge between Asp-33 in E5 protein and Lys-499 in PDGFβR, (*c*) a hydrogen bond between Gln-17 in E5 and Thr-513 in the PDGFβR TMD, and (*d*) an E5 homodimer interface related to the interface identified by genetic analysis. (*ii*) We excluded clusters with improper membrane insertion or the presence of gross helical kinks. (*iii*) We also excluded clusters not found when the modeling was conducted with the closely related E5 sequences of homologous ungulate fibropapillomaviruses (deer, sheep, and Western roe deer). Finally, we reasoned that active BPV E5 mutants should also adopt the correct structure. To explore this, we repeated the Rosetta modeling with E5 variants, Q17S, Q17W, LRM4, and LRM19, each of which retains activity with the PDGFβR (22, 23). We identified only one cluster, 33.1, that satisfied all these criteria, which served as the starting point for MD simulations.

All-Atom MD Simulations of E5–PDGFβR Complexes. To understand the likely arrangements and chemical interactions of the transmembrane helices in the complex of the PDGFβR and the BPV E5 protein, we added amino acid side chains to the Rosetta model, placed it in a hydrated lipid bilayer, and refined it by all-atom MD

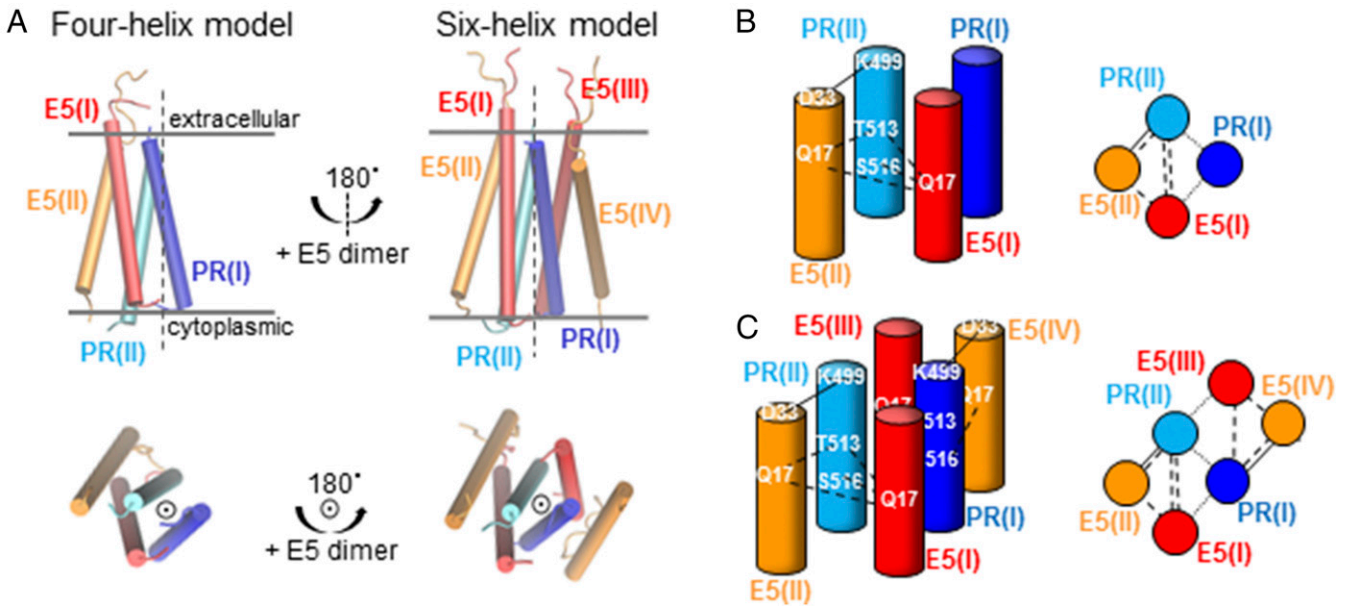

Fig. 2. Interaction cartoon and overall structure of the four- and six-helix models of E5-PDGFβR complexes obtained by MD simulations. (*A*) Structures of the two models obtained by MD simulations. Alpha-helices are represented as cylinders. To construct the six-helix model (*A*, *Right*), the E5 dimer [E5(I) and E5(II)] in the four-helix model (*A*, *Left*) was rotated by 180° around the axis indicated by the vertical dashed line (*A*, *Upper*) or the point (*A*, *Lower*), thereby generating E5(III) and E5(IV). The entire complex was then subjected to MD simulation. E5(I) and E5(III) domains are in orange, E5(II) and E5(IV) domains are in red, PR(I) domain is in dark blue, and PR(II) domain is in light blue. (*B* and *C*) Cartoon representation of the four-helix (*B*) and six-helix (*C*) models where each cylinder represents a separate TMD, color coded as in *A*. Salt bridges are represented by the solid lines, hydrogen bonds are indicated by the dashed lines, and packing interactions are indicated by the dotted lines. For clarity, disulfide bonds between the E5 monomers are not shown, nor are all other interactions. *B* and *C*, *Left*, lateral view. *B* and *C*, *Right*, axial view from extracellular position.

simulations to ensure chemically realistic, energetically favorable helix orientations and packing of the side chains in the structure. An MD simulation of the initial complex was run for 120 ns in a hydrated 1-palmitoyl-2-oleoyl-*sn*-glycero-3-phosphocholine (POPC) lipid bilayer. The structure was stable during the simulation run, with a backbone atom root-mean-square deviation (rmsd) relative to the initial structure of ∼1.55 Å (Fig. S2*A*).

In the refined four-helix model, the E5 dimer and the two PDGFβR TMDs both adopted left-handed crossing angles. The E5 dimer was stabilized by a Cys-39–Cys-39 disulfide bond at the C terminus of the E5 segment and by a Gln-17–Gln-17 hydrogen bond in the membrane center, as well as by numerous van der Waals (vdW) contacts (four-helix model in Fig. 2 *A* and *B*). Interestingly, the simulation indicated that the arrangement of the PDGFβR TMDs relative to the E5 dimer was not symmetric: One of the PDGFβR TMDs [PR(II)] interacted extensively with both E5 helices, whereas the other PDGFβR TMD [PR(I)] interacted with only one E5 monomer [E5(I)] via packing interactions (Fig. 2*B*). Gln-17 residues in E5(I) and E5(II) were hydrogen-bonded to Thr-513 of PR(II), as well as to each other. The interaction between the E5 dimer and PR(II) was also stabilized by an E5(I) Gln-17–PR(II) Ser-516 hydrogen bond and an E5(II)–Asp-33–PR(II) Lys-499 salt bridge. These bonds, as well as tight packing of hydrophobic residues within the complex, resulted in strong interactions among E5(I), E5(II), and PR(II), whereas PR(I) interacted only with E5(I) and PR(II). The vdW interaction energy between the two PDGFβR TMDs in the four-helix model was −27.9 kcal/mol (Fig. 3*A*, red line, and Table S1), and the average backbone rms fluctuations (rmsf) of the PR(I) and PR(II) domains were 1.71 and 1.37 Å, respectively (Fig. 3*B*, red symbols, and Table S1), with the least fluctuation in the middle of the membrane.

The loose association of PR(I) TMD in the four-helix model suggested that there might be other arrangements of the TMDs with greater stability. Therefore, MD simulations were used to interrogate additional models with different subunit stoichiometry. Inspection of the four-helix complex suggested the possibility of a six-helix complex consisting of a dimer of the PDGFβR TMD sandwiched between two E5 dimers. In this model, each E5 dimer interacted primarily with a different PDGFβR TMD, producing a relatively symmetrical "dimer of trimers" complex (Fig. 2 *A* and *C*). The interaction between two PDGFβR TMDs was not fully symmetrical. PR(I) residues Leu-509, Leu-512, Ile-515, Ile-519, Met-522, Lys-526, Lys-527, and Pro-528 engaged in vdW contacts with PR(II) residues Ser-504, Ala-508, Leu-512, Ile-515, Ile-518, Ile-519, Met-522, and Gln-525 (Fig. 3*C* and Table S2). The simulations indicated that this six-helix complex was favored, with a vdW interaction energy between the two PDGFβR TMDs of −35.5 kcal/mol (compared with −27.9 kcal/mol in the four-helix model) (Table S1 and Fig. 3*A*,

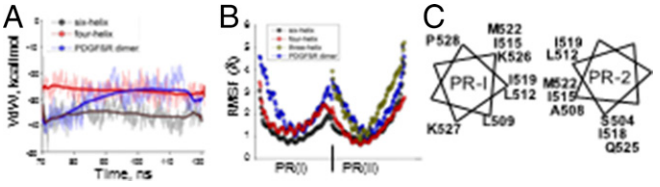

Fig. 3. E5 dimers restrict the dynamics of the PDGFβR TMD dimer and increase its stability. (*A*) vdW interaction energies between the PDGFβR TMDs calculated for the last 50 ns of MD trajectory for the six-helix (gray), four-helix (red), and PDGFβR dimer (blue) models. Lower energies correspond to better vdW packing. (*B*) RMSF scan along the last 50 ns of MD trajectory for the PDGFβR TMDs for the six-helix (gray), four-helix (red), three-helix (one E5 dimer and one molecule of the PDGFβR TMD) (yellow), and PDGFβR dimer (blue) models. Each symbol represents an individual backbone N, O, or Cα carbon. The most flexible elements are at the ends of the TMDs at membrane interfaces. The least flexible elements are in the center of the membrane. (*C*) Helical wheel diagram of the PDGFβR TMD dimer in the six-helix model, with the residues interacting in the interface labeled.

black line), and with lower backbone fluctuation in the PDGFβR TMDs [the average rmsf of the PR(I) and PR(II) domains were 1.24 and 1.42 Å, respectively (Table S1 and Fig. 3*B*, black symbols)]. The rmsd of the PDGFβR TMD backbone atoms was 1.7–2.5 Å relative to the initial structure (Fig. S2*A*). In the six-helix model, each PDGFβR TMD interacted with its corresponding E5 dimer through hydrogen bonding (Gln-17–Thr-513 and Gln-17–S516) in the center of the membrane, through a salt bridge (Asp-33–Lys-499) at the membrane–water interface, and through hydrophobic packing interactions (Fig. 2*C* and Table S2). The detailed structure and main interactions of the hexameric complex are shown in Fig. 4. A list of all hydrogen bonds and salt bridges computed during the last 50 ns of simulation is presented in Table S3, and a full contact map between the different segments of the complex is given in Dataset S1.

We also studied parts of the six-helix model in isolation: a dimer of the PDGFβR TMDs in the absence of the E5 protein and a three-helix complex consisting of the E5(I)–E5(II) dimer and the PR(II) TMD. Each of these complexes was stable during the simulation runs. For the isolated PDGFβR dimer, the vdW interaction energy between the two PDGFβR TMDs was −31.9 kcal/mol, and the average rmsf values of the PR(I) and PR(II) domains were 2.22 and 2.14 Å, respectively (Table S1). In the three-helix complex, the average rmsf of the PR(II) domain was 2.39 Å (Table S1). These results indicate that the PDGFβR TMDs have the strongest vdW interactions and the smallest fluctuations in a six-helix E5–PDGFβR complex consisting of two E5 dimers embracing a dimer of the PDGFβR TMD. Stabilizing H bonds were noted in the structure (Table S3) and suggested by experimental evidence (6, 23). In the six-helix model, each E5 dimer interacted with the TMDs of two receptor molecules, helping to stabilize the receptor dimer and orienting the two receptor TMDs to favor the active state. These effects would not be expected if E5 were monomeric, since the intrinsic stability of the E5 dimer provides additional energy that stabilizes the dimer of the PDGFβR TMDs. The presence of two E5 dimers in the six-helix model takes advantage of the approximate twofold symmetry to further stabilize the complex.

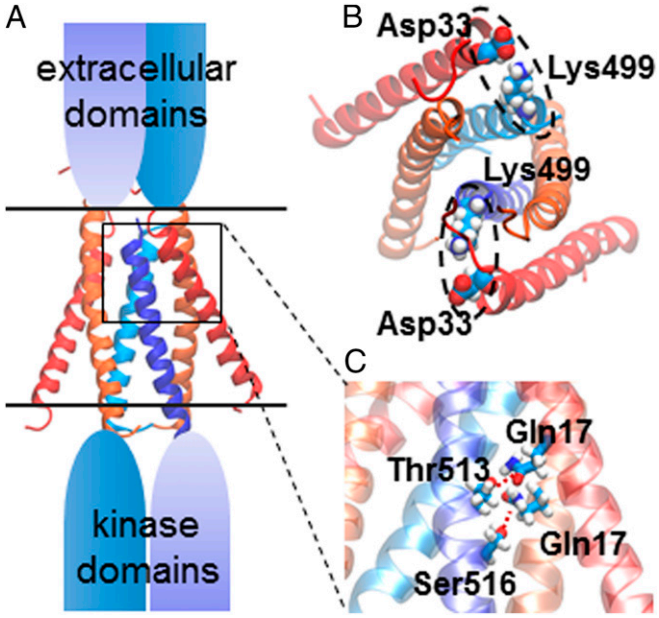

Fig. 4. All-atom structure of six-helix complex obtained by MD simulations. (*A*) Ribbon diagram overview of the six-helix model viewed from the side. The horizontal lines represent the approximate boundaries of the membrane. The PDGFβR is shown in blue, with the extracellular ligand binding and intracellular kinase domains represented by the ovals attached to the TMDs. E5 proteins are shown in red and orange. (*B*) Axial view of the complex. Salt bridges between Asp-33 and Lys-499 for E5(II) and PR(II) and for E5(IV) and PR(I) are circled. (*C*) Enlargement of a side view of the complex showing side chains of residues participating in hydrogen bonds involving E5(I), E5(II), and PR(II) in the middle of the TMDs. E5(II) and E5(IV) are colored red.

Mapping Faces of the PDGFβR Transmembrane Domain Required for E5 Action. We tested the most salient features of the six-helix model. First, we tested a set of seven PDGFβR mutants to explore which amino acids in the TMD of the PDGFβR are required for a productive interaction with the E5 protein. In each mutant, the amino acids spaced every seventh position in the TMD were replaced by alanine (or with leucine at positions 505 and 508, which are alanine in wild type) (Fig. 5*A*). If the PDGFβR TMDs in the active complex have a left-handed crossing angle [as suggested by the modeling conducted here and by NMR experiments on a PDGFβR peptide (29)], the substitutions in each mutant fall on a single face of the TMD. Mutations that lie in the PDGFβR/E5 interface are likely to disrupt the interaction of the E5 dimer(s) with the PDGFβR. The PDGFβR face mutants are designated PRFM1 through PRFM7. Each mutant was stably expressed in murine BaF3 cells, which do not express endogenous PDGFβR and are dependent on interleukin-3 (IL-3) for proliferation. Activation of an exogenous PDGFβR by the E5 protein allows BaF3 cells to proliferate in medium lacking IL-3 (26).

BaF3 cells expressing each receptor mutant were transduced separately with the E5 gene or v-*sis*, a homolog of PDGF, which binds the extracellular domain of the receptor. IL-3 independence was scored as a measure of the ability of E5 and v-*sis* to cooperate with the PDGFβR mutants. As shown in Fig. 5*B*, the E5 protein and v-*sis* were highly active with wild-type PDGFβR and PRFM1, 2, and 5, implying that the amino acids on these faces did not play a crucial role in E5 activity. PRFM6 was moderately defective with v-*sis* and at least as active with E5, implying that face 6 was also not important for E5 activity. In contrast, the activity of the E5 protein was significantly reduced in cells expressing PRFM3 or 7, even though both mutants responded robustly to v-*sis*, showing that these two faces were important for E5 action. PRFM4 did not respond well to either E5 or v-*sis*, so we cannot state whether this face is important for E5 action or whether the intrinsic signaling activity of this receptor mutant is impaired.

To confirm that the E5 protein failed to activate the defective PDGFβR mutants, detergent extracts of cells coexpressing the E5 protein and the wild-type PDGFβR or the PRFM mutants were immunoprecipitated with the anti-PDGF receptor antibody and immunoblotted with an anti-phosphotyrosine antibody. As shown in Fig. 5*C*, the E5 protein caused tyrosine phosphorylation of the wild-type PDGFβR, as well as of PRTM1, 2, 5, and 6, but displayed markedly reduced ability to induce phosphorylation of the defective mutants PRTM3 and 7, as well as of PRTM4. Thus, alanine mutations on these faces of the PDGFβR TMD disrupted the productive interaction between the E5 protein and the PDGFβR and inhibited biological activity.

In the six-helix model, the residues mutated in PRFM3 and 7 make numerous contacts with both E5 dimers (Table S2). In addition, PRFM4 in PR(I) makes numerous contacts with the E5(III)/E5(IV) dimer. These contact residues include Thr-513 on face 7 and Ser-516 on face 3, which hydrogen-bond to both E5 dimers. In fact, seven of the eight residues in PR(II) that are predicted to contact E5(II) lie on face 3, 4, or 7, as do all eight residues in PR(I) predicted to contact E5(III). Conversely, of the 12 predicted contacts between the two PDGFβR TMDs spanning amino acids 500–524, only residue 509 in face 3 of PR(II) is mutated in PRFM3, 4, or 7. These results support the six-helix model by providing an explanation for the inability of the defective receptor mutants to respond to the E5 protein.

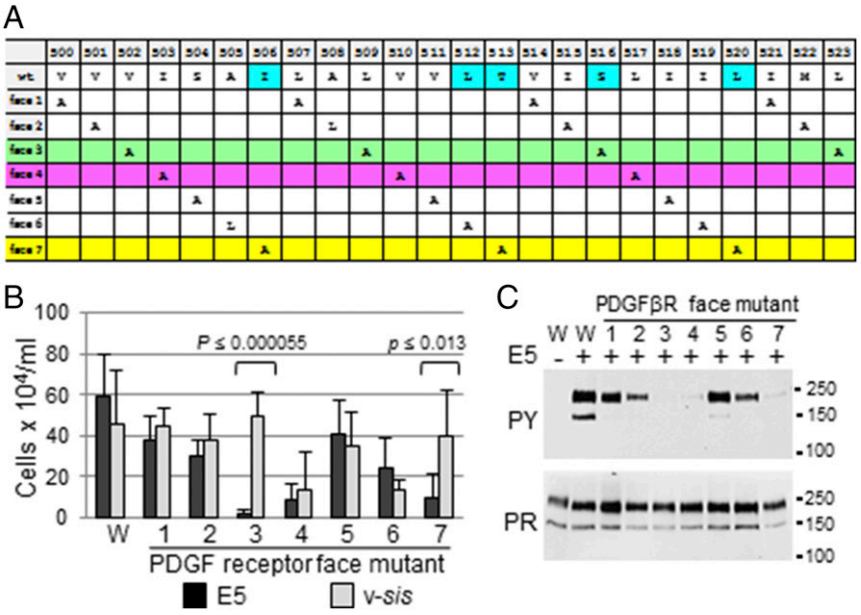

Fig. 5. Identification of PDGFβR TMD residues required for E5 action. (*A*) Chart showing the set of seven PRFM mutants. Top row shows the position of amino acids in the murine PDGFβR TMD sequence. Second row shows the sequence of the wild-type murine PDGFβR, with residues previously implicated in E5 binding highlighted light blue. Other rows show the substitutions in each of the seven PRFM mutants. The two faces shown to be important for activity (*B*) are colored green (face 3) and yellow (face 7). Face 4 is colored purple. An empty cell indicates that the mutant contains the wild-type amino acid at that position. (*B*) BaF3 cells expressing the wild-type PDGFβR or the indicated PRFM mutant were infected with MSCVp or with MSCVp expressing the wild-type BPV E5 protein or v-*sis*. After selection for puromycin resistance, cells were incubated in medium lacking IL-3. The average number of viable cells 6 or 7 d after IL-3 removal is shown for E5 (black bars) and v-*sis* (gray bars). The background number of IL-3–independent cells after transduction of MSCVp was subtracted in each experiment. Each receptor mutant was tested with E5 and v-*sis* in at least five independent experiments. Statistical significance of the results was determined by using a Welch's two-tailed *t* test with unequal variances. (*C*) Detergent extracts were prepared from BaF3 cells expressing the wild-type PDGFβR (W) or the indicated PRFM mutant in the presence (+) or absence (–) of the E5 protein. Extracts were immunoprecipitated with anti-PDGF receptor antibody, subjected to gel electrophoresis, and immunoblotted with anti-PDGF receptor antibody (*C*, *Lower*) to detect total PDGFβR and with anti-phosphotyrosine antibody (*C*, *Upper*) to detect PDGFβR tyrosine phosphorylation. Similar results were obtained in three independent replicate experiments.

Biochemical Evidence that the PDGFβR Transmembrane Domain Recruits More than One E5 Dimer into the Complex. The fundamental feature of the six-helix model is the presence of two E5 dimers and two PDGFβR TMDs in the complex. To test this feature of the model, we performed coimmunoprecipitation experiments to determine whether two differentially tagged E5 dimers coexist in a complex with the PDGFβR TMD. E5 proteins containing an N-terminal HA or FLAG epitope tag were used for these experiments (Fig. S2*B*). FLAG-tagged E5 also contained a 23-amino acid *Saccharomyces cerevisiae* Put3 dimerization domain inserted between the epitope tag and the E5 sequence to increase its size relative to the HA-E5 protein. Both HA-E5 and FLAG-Put3–E5 retained transforming activity. HA-E5, FLAG-Put3–E5, or both were stably expressed in BaF3 cells. SDS/PAGE under reducing and nonreducing conditions followed by immunoblotting with anti-HA or -FLAG antibody demonstrated that the monomeric and dimeric forms of the differentially tagged E5 proteins have distinct electrophoretic mobilities (Fig. S2*C*). In cells coexpressing the two tagged E5 proteins, the anti-FLAG antibody coimmunoprecipitated HA-E5 detectable as a monomeric species on a reducing gel (Fig. S2*D*, lane 5), suggesting that heterooligomers between HA-E5 and FLAG-Put3–E5 form in the absence of the PDGFβR.

To determine whether HA-E5 and FLAG-Put3–E5 homodimers coexist in a complex with the PDGFβR, we analyzed BaF3 cells stably expressing one or both E5 proteins in the presence or absence of wild-type PDGFβR. Direct immunoblot analysis of the input cell lysates demonstrated that homodimers of HA-E5 and homodimers of FLAG-Put3–E5 were expressed in the appropriate cell lines (Fig. S3*A*), and anti-FLAG immunoprecipitation followed by anti-PDGF receptor immunoblotting confirmed that the FLAG-Put3–E5 protein stably associated with PDGFβR (Fig. S3*C*, lane 6). To determine whether both E5 dimers were present in the complex, we performed anti-FLAG immunoprecipitation followed by SDS-gel electrophoresis under nonreducing conditions to dissociate the E5 protein from the PDGFβR while keeping disulfide-linked E5 dimers intact, followed by immunoblotting with anti-HA or -FLAG antibody. As expected, the anti-FLAG antibody precipitated abundant FLAG-Put3–E5 homodimer (as well as a smaller amount of monomeric FLAG-Put3–E5), whether or not the cells expressed the PDGFβR (Fig. 6, *Right*, lanes 2 and 3). In cells expressing both differentially tagged E5 proteins, the FLAG antibody did not precipitate the HA-E5 homodimer from extracts lacking the PDGFβR (Fig. 6, *Left*, lane 2), demonstrating that anti-FLAG did not cross-react with HA-E5 and that that HA-tagged E5 homodimers did not associate with FLAG-tagged E5 homodimers in the absence of the PDGFβR. Importantly, the anti-FLAG antibody coimmunoprecipitated the HA-E5 homodimer from extracts of cells expressing both of the E5 dimers and the PDGFβR (Fig. 6, *Left*, lane 3). Thus, coimmunoprecipitation of the HA-E5 homodimer with an antibody recognizing only the FLAG-tagged E5 homodimer required the presence of the PDGFβR. These results show that the PDGFβR promotes the assembly of a complex containing FLAG-Put3–E5 and homodimers of HA-E5, as predicted by the six-helix model.

In extracts of cells expressing both E5 proteins, whether or not the PDGFβR was present, the anti-FLAG antibody immunoprecipitated an anti–HA-immunoreactive protein with an electrophoretic mobility on nonreducing gels between that of HA-E5 homodimers and FLAG-Put3–E5 homodimers (Fig. 6, *Left*, lanes 2–4, marked with an asterisk). This protein most likely is a heterodimer between HA-E5 and FLAG-Put3–E5. This heterodimeric protein was not detected when anti-FLAG was used to probe a

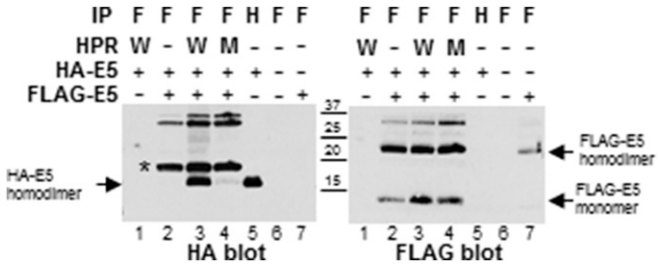

Fig. 6. PDGFβR recruits more than one E5 dimer into the receptor/E5 protein complex. Detergent extracts were prepared from BaF3 cells expressing the wild-type (W) or T513L (M) human PDGFβR (PR) or no PDGFβR (–); the HA-tagged E5 protein; or the FLAG-tagged Put3–E5 protein, as indicated. Extracts were immunoprecipitated (IP) with anti-FLAG (F) or anti-HA (H) antibody as indicated and electrophoresed on a nonreducing denaturing gel to disrupt noncovalent complexes while maintaining disulfide-linked E5 dimers. After transfer, the filter was probed with anti-HA antibody (*Left*) and then stripped and reprobed with anti-FLAG antibody (*Right*). The size of mobility markers (in kilodaltons) is shown in the center. Bands representing the monomeric and dimeric forms of the tagged E5 proteins are shown with arrows. The band marked with * in the HA blot appears to be a heterodimer between HA- and FLAG-tagged E5. Similar results were obtained in three independent replicate experiments.

nonreducing gel, suggesting that the anti-FLAG antibody is not able to recognize FLAG-Put3–E5 in the heterodimer by immunoblotting. Higher-molecular-mass HA-immunoreactive proteins were also present in the anti-FLAG immunoprecipitates from cells expressing FLAG-Put3–E5, which may represent higher-order oligomeric complexes that are not dependent on PDGFβR.

We next determined whether the coexistence of both E5 homodimers in a complex requires interaction between the PDGFβR and the E5 protein. We used a mutant PDGFβR containing a threonine-to-leucine substitution at position 513 (T513L) in the TMD, which prevents the association between the E5 protein and the PDGFβR (31). We analyzed BaF3 cells expressing the two differentially tagged E5 proteins and either the wild-type or T513L mutant PDGFβR. The mutant receptor was expressed at a similar level as the wild-type receptor, but, as expected, did not interact with the FLAG-Put3–E5 protein (Fig. S3*C*, lane 7). Notably, the anti-FLAG antibody coimmunoprecipitated little HA-E5 homodimer from extracts of cells expressing the PDGFβR mutant, compared with the abundant amount precipitated from cells expressing the wild-type PDGFβR (Fig. 6, *Left*, compare lanes 3 and 4). Thus, a physical interaction between the E5 protein and the TMD of the PDGFβR is required for the coexistence of both E5 dimers in the complex, as predicted from the six-helix model.

We also determined whether the TMD of the PDGFβR was sufficient for recruiting multiple E5 dimers into the complex. We used a doubly truncated PDGFβR, TMPR, which consists primarily of the TMD because it lacks both intracellular and extracellular domains (Fig. S2*B*) (18). BaF3 cells stably expressing similar levels of HA-E5 and FLAG-Put3–E5 were established in the absence or presence of the full-length PDGFβR or TMPR containing a wild-type TMD or a T513L mutant TMD (Fig. S3*B*). As expected, TMPR interacted with the E5 protein, and binding was eliminated by the T513L mutation (Fig. S3*D*). As shown in Fig. 7 (*Left*), anti-FLAG antibody coimmunoprecipitated a substantial amount of the HA-E5 homodimer from cells expressing TMPR or the full-length receptor (lanes 2 and 4), but not from cells expressing the T513L TMPR mutant (lane 5). Thus, a PDGFβR TMD competent to bind to E5 is sufficient to recruit more than one E5 dimer into the complex. Evidence that the active complex contains, in fact, two E5 dimers is presented below.

Determining the Stoichiometry of the E5/PDGFβR Transmembrane Complex by Native Gel Electrophoresis. To determine the size of the complex between the E5 protein and the PDGFβR, we conducted electrophoresis experiments with blue native gels. This system uses Coomassie blue G-250, which imposes a negative charge on proteins without denaturation, thereby enabling separation by electrophoresis based on size, while maintaining the native associations of protein complexes (33, 34). This technique is particularly suitable for analysis of membrane protein complexes because Coomassie blue binds well to hydrophobic proteins in the presence of a mild detergent and reduces their tendency to aggregate (33, 34). For these experiments, we used BaF3 cells expressing the HA-E5 protein and the truncated TMPR PDGFβR, which contains the C-terminal epitope recognized by the PDGFβR antibody (18). TMPR was studied to prevent cellular proteins from binding to the PDGFβR intracellular domain and affecting the mobility of the complex. Immunoblotting with anti-PDGFR antibody detected TMPR not in complex with E5 as a faint, rapidly migrating band in the presence or absence of the E5 protein (Fig. S4*B*, *Left* and *Center*), which was run off the gel in some experiments to better resolve the larger complexes. When HA-E5 and TMPR were coexpressed and analyzed by blue native polyacrylamide gel electrophoresis (BN-PAGE), anti-PDGFβR antibody detected a single prominent band with an apparent molecular mass of ∼60 kDa relative to soluble globular protein standards (Fig. 8*A*, lanes 11 and 13). This band was present only when HA-E5 and TMPR were coexpressed, and it was not present if TMPR harbored the T513L mutation that prevented E5 binding (Fig. 8*A*, lane 12) or if the samples were treated with reducing agents before electrophoresis (Fig. 8*A*, lane 14), which dissociated the disulfide-linked E5 dimer, thereby eliminating complex formation and resulting in the appearance of a more rapidly migrating form (Fig. S4*B*, *Right*). A band with the same mobility was detected by anti-HA antibody only when HA-E5 and TMPR were coexpressed (Fig. 8*A*, lane 5). We conclude that this band is the complex between TMPR and at least one HA-E5 dimer.

A six-helix complex consisting of two HA-E5 dimers and two molecules of TMPR (without a signal peptide) has a predicted molecular mass of 40 kDa, whereas the molecular mass of a four-helix complex containing a single HA-E5 dimer would be 26.2 kDa. To estimate the size of the E5/PDGFβR complex, we used a series of small transmembrane protein standards to calibrate the blue native gels, including a chimeric FLAG-APEX–E5 protein and various oligomeric forms of an HA-tagged four-helix snake consisting of two E5 TMDs linked to two PDGFβR TMDs in alternating order (predicted monomeric size, 23.7 kDa) (*Materials and Methods* and Fig. S4*C*). These proteins were

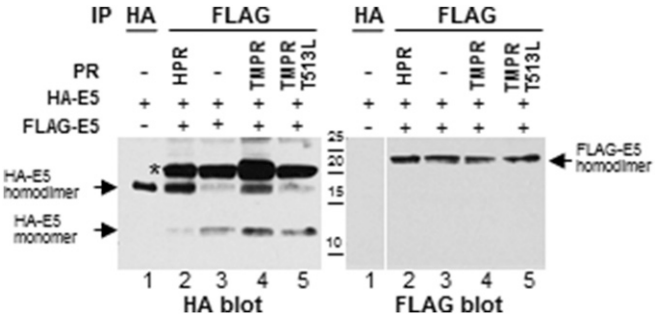

Fig. 7. PDGFβR TMD is sufficient to recruit more than one E5 dimer into the complex. Samples were prepared and processed as described in the legend to Fig. 6, except that the receptors tested were full-length human PDGFβR (HPR), the doubly truncated TMPR PDGFβR, or TMPR containing a Thr to Leu mutation at position 513 in the middle of the receptor TMD. The size of mobility markers (in kilodaltons) is shown in the center. Bands representing the monomeric and dimeric forms of the tagged E5 proteins are shown with arrows. The band marked with * in the HA blot appears to be a heterodimer between HA- and FLAG-tagged E5. Similar results were obtained in three independent replicate experiments.

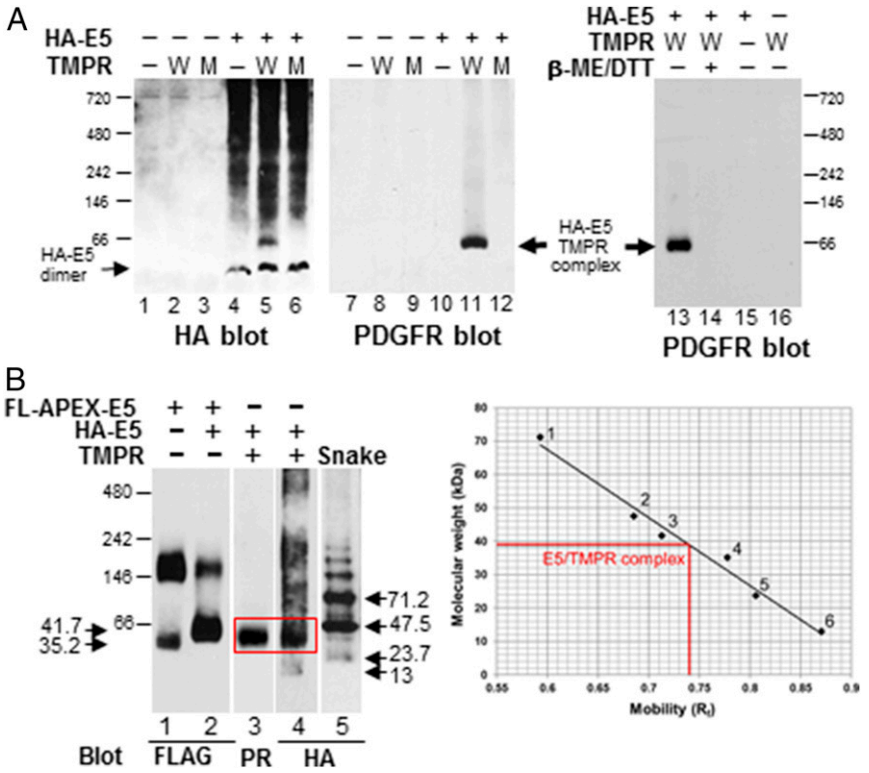

Fig. 8. Analysis of the E5/PDGFβR complex by blue native gel electrophoresis. (*A*) Detergent extracts were prepared from BaF3 cells expressing no PDGFβR (–) or TMPR with a wild-type (W) or T513L mutant (M) TMD. In addition, cells expressed HA-E5, as indicated. A, *Left* and *Center* show proteins electrophoresed on the same blue native gel and probed sequentially with anti-HA and anti-PDGF receptor antibodies. *A*, *Right* shows similar samples incubated in 0.1% SDS in the presence (+) or absence (–) of reducing agents β-mercaptoethanol and DTT (β-ME/DTT), electrophoresed on a blue native gel, and probed with anti-PDGF receptor antibody. The thin and thick arrows indicate the positions of the HA-E5 dimer and the complex between HA-E5 and TMPR, respectively. Size (in kilodaltons) of soluble molecular mass standards is shown. Similar results were obtained in three independent replicate experiments. A darker exposure of lanes 13–16 is shown in Fig. S4*B*, *Right*. (*B*) Extracts of cells expressing the indicated proteins were electrophoresed on the same blue native gel and blotted sequentially with anti-HA and -FLAG antibodies to detect the TMD molecular mass standards and with anti-PDGF receptor antibody to detect the HA-E5/TMPR complex (shown in red box). Individual lanes were cropped from the same gel and aligned. The original images are shown in Fig. S4*A*. The labeled arrows show the predicted molecular mass of the TMD standards listed in Fig. S4*C*. The graph plots the mobility (R_f; distance migrated/length of the gel) of these standards vs. their predicted molecular mass in a representative experiment. The mobility and estimated molecular mass of the HA-E5/TMPR complex electrophoresed on the same gel as these standards is shown by red lines. Similar results were obtained in three independent replicate experiments.

expressed in BaF3 cells, separated by BN-PAGE, and detected by immunoblotting to construct a standard curve (Fig. 8*B*, *Right*). As shown in the red box in Fig. 8*B*, *Left*, the complex detected by the anti-PDGF receptor antibody and the HA antibody migrated between the 35.2-kDa monomeric FL-Apex–E5 and the 41.7-kDa HA-E5/FL-Apex–E5 heterodimer bands. The estimated molecular mass of the complex based on three independent experiments was 38.6 kDa (Fig. 8*B*, *Right*), in excellent agreement with 40 kDa, the predicted size of the six-helix complex, and considerably larger than the predicted size of the four-helix complex (26.2 kDa). These data provide biochemical evidence that the complex in mouse cells contains two PDGFβR TMDs and two copies of the HA-E5 homodimer.

Discussion

Prior genetic and biophysical studies showed that the dimeric E5 protein interacts directly with the TMD of the PDGFβR, resulting in receptor dimerization, activation, and cell transformation. Better understanding of this process promises to provide new insights into the nature and consequences of protein–protein interactions occurring in membranes. However, the high-resolution structure of the signaling complex between the E5 protein and the TMD of the PDGFβR is not known because determining the structure of TMD complexes in the active state in the membrane poses significant experimental challenges. To circumvent this problem, we have developed an approach that uses experimental data to constrain the ab initio structural prediction of the complex by using Rosetta modeling, followed by all-atom MD simulations to develop a chemically detailed computational model and to guide the design of genetic and biochemical experiments to test key features of the model. In the modeling conducted here, we first converted the interacting TMDs into a single snake-like molecule in silico and considered a complex consisting of one E5 dimer and two molecules of the PDGFβR (4, 6, 9, 12, 23). Our modeling revealed an unexpected disposition of the PDGFβR TMDs within the four-helix complex that led us to consider alternative stoichiometries. Based on further computational, genetic, and biochemical analysis, we propose a model for the E5/PDGFβR complex in which there are two E5 dimers in the active complex.

The E5 protein is a dimer even in cells lacking the PDGFβR, and E5 dimerization is required for receptor binding and activation (7, 11, 25). We previously used chimeric fusion proteins to map the homodimer interface within the active E5 dimer (11). This analysis, which assumed that the E5 dimer was symmetric, identified two related interfaces with a left-handed crossing angle that conferred transforming activity on the chimeras. The interface of the most active chimera (chimera V: Ala-14, Gln-17, Leu-21, Leu-24, and Phe-28), which was used in selecting Rosetta cluster 33.1, was also identified by prior MD simulations

of the E5 dimer and by solution-state NMR studies of peptides corresponding to the E5 TMD in SDS micelles (9, 23). Chimera I (interfacial amino acids Val-13, Gln-17, Leu-20, Leu-24, and Leu-27) also displayed significant biological activity (11). The homodimer interfaces in the two E5 dimers in the six-helix model were similar to each other, but not identical and not strictly symmetric (Fig. 9). Specifically, Val-13, Gln-17, Leu-18, Leu-21, Leu-24, Phe-27, and Tyr-31 made interhelical contacts in the interfaces of both E5 dimers, whereas Ala-14, Met-16, and Phe-23 made contacts in the E5(I)/E5(II) dimer only, and Leu-20 and Phe-28 made contacts in the E5(III)/E5(IV) dimer only (Table S2). Fig. 9 shows helical wheel diagrams illustrating that the E5 homodimer interfaces in the six-helix model are comprised almost exclusively of amino acids found in the two interfaces defined by the chimeric protein approach. The close similarity of the experimentally defined and modeled E5 homodimer interfaces provides an additional test of the six-helix model. It is possible that the E5 protein initially dimerizes symmetrically and that binding to the PDGFβR TMDs causes slight shifts in the E5 homodimers to generate the interfaces predicted by the six-helix model.

The E5 dimer is thought to activate the PDGFβR by stabilizing the interaction of two PDGFβR TMDs in an orientation that results in the correct positioning of the linked intracellular kinase domains to stimulate kinase activity (17). To assess the relative stability of the PDGFβR TMD dimers in the different models, we examined the average vdW interaction energy between the two PDGFβR TMDs and the average rmsf of the backbone atoms in each PDGFβR helix. More stable associations should have lower (more negative) interaction energies and reduced internal fluctuations. The six-helix complex consisting of two E5 dimers and a dimer of the PDGFβR TMD was the most favorable by both of these criteria. In the four-helix complex, PR(I) fluctuated more than PR(II) because it was not tethered in place by the second E5 dimer, which would limit the dynamics of PR(I). The PDGFβR TMDs also exhibited higher fluctuations in the three-helix complex and the PDGFβR TMD dimer complex. For all complexes, the highest rmsf values were at the ends of the sequences (the membrane interface regions), whereas the membrane-buried residues exhibited lower fluctuations (Fig. 3*B*). The least mobile residues in the receptor TMD were located in the center of the membrane and included Ile-506, Leu-509, Leu-512, and Thr-513; their relative immobility suggests that they are likely to be key to TMD dimerization, which is consistent with prior mutational analysis (22, 27, 30). The PDGFβR TMD residues flanking these central residues also underwent less fluctuation when engaged by the two E5 dimers (Fig. 3*B*). Similarly, the vdW interaction energy between the two PDGFβR TMDs was lowest when the PDGFβR dimer was confined by the two E5 dimers (Table S1). Thus, the vdW energies and the fluctuation data argue for a better packing of PR(I) and PR(II) domains in the six-helix complex, with two E5 dimers embracing a single PDGFβR dimer, than in the four-helix interaction. We point out that this favorable energy in the six-helix complex was calculated for the vdW interactions between the two PDGFβR TMDs only, and does not take account of additional interactions that stabilize TMD dimer formation.

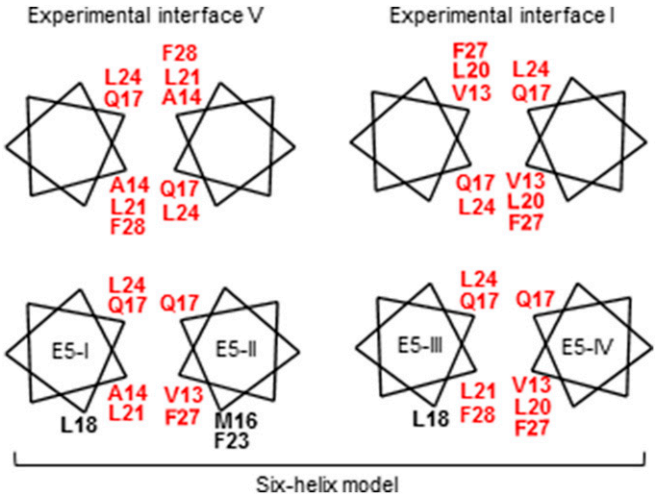

Fig. 9. Helical wheel diagrams of the E5 dimer. *Upper* shows the amino acids lining the symmetric E5 homodimer interfaces inferred from analysis of active chimeric E5 proteins (11). *Lower* shows the two E5 dimers in the six-helix model, with amino acids that make interhelical contacts across each E5 dimer interface shown. Amino acids that form contacts in both the six-helix model and in either of the two experimentally determined interfaces are shown in red. Note that Ala-14, Met-16, and Phe-23 stabilize the E5(I)/E5(II) dimer only and Leu-20 and Phe-28 stabilize the E5(III)/E5(IV) dimer only. In all diagrams, amino acids only between positions 10 and 30 are shown.

The interface between the two PDGFβR TMDs in the six-helix model is similar to the interface determined by NMR of a PDGFβR TMD dimer in the absence of the E5 protein (29). This NMR structure, in turn, appears consistent with the low-resolution structure of the full-length PDGFβR dimer activated by PDGF binding, as determined by negative-stain electron microscopy (15). The two PDGFβR TMDs in the six-helix model do not display twofold symmetry (Fig. 3*C*). However, it is important to note that transphosphorylation is intrinsically asymmetric, since one receptor molecule in the dimer phosphorylates the other, so it is not surprising that the favored receptor dimer lacks perfect twofold symmetry.

In the six-helix model, the interaction of the PDGFβR TMDs with two E5 dimers are not equivalent, with one E5 dimer interacting primarily with faces 3 and 7 of the PDGFβR TMD, and the other dimer with faces 3, 4, and 7. Consistent with the model, alanine scanning mutagenesis identified faces 3 and 7 of the PDGFβR TMD as being most important for PDGFβR activation in response to the E5 protein. Leu-512 in the PDGFβR TMD is also important for the interaction of the E5 protein with the PDGFβR, as revealed by the defect caused by a leucine-to-isoleucine substitution at this position (22). Position 512 was not identified as being important by alanine scanning mutagenesis, presumably because the interaction between the E5 protein and the PDGFβR was not disrupted by alanine at this position in PRTM6. In our model, Leu-512 in each PDGFβR TMD made vdW contacts with one of the E5 monomers and with the other PDGFβR TMD, thereby providing additional packing contacts that stabilized the complex.

Most critically, analysis of the E5/PDGFβR complex isolated from cells provided a biochemical test of the six-helix model. We showed by coimmunoprecipitation that two E5 dimers coexist in the complex only when the PDGFβR TMDs are present and competent to bind the E5 protein. Indeed, the TMD of the PDGFβR was sufficient to recruit the two E5 dimers into the complex. In addition, the electrophoretic mobility of the native complex eliminated the possibility that it is a four-helix complex and strongly suggested that it consists of a pair of E5 dimers and two PDGFβR TMDs. The appearance of a single band reactive with anti-PDGFR antibody in the native gel analysis under non-reducing conditions indicated that the six-helix complex does not propagate into higher-order disulfide-linked oligomeric forms.

Prior studies suggested the existence of a salt bridge between E5 Asp-33 and PDGFβR Lys-499, a hydrogen bond between E5 Gln-17 and PDGFβR Thr-513, and hydrogen bonds between Gln-17 on the two E5 monomers. These constraints were used to select the original four-helix Rosetta model and persisted in the six-helix model after MD refinement. In addition, earlier mutational analysis revealed the importance of several other

residues in the PDGFβR TMD, including Ile-506 and Leu-509 (18, 22, 30, 31), which is consistent with the analysis of the PDGFβR face mutants and with the six-helix model, which predicts that these residues make direct contacts with the E5 protein (Tables S2 and S3).

The six-helix model provides insights into two important questions: How does E5 binding promote dimerization of the PDGFβR, and why is dimerization of the E5 protein required for activity? In addition to vdW packing interactions between the two PDGFβR TMDs, the six-helix complex is further stabilized by a complex web of disulfide bonds, salt bridges, hydrogen bonds, and vdW interactions involving the E5 proteins. Notably, although each E5 dimer binds primarily to a single PDGFβR TMD, there are also vdW interactions between one monomer in each E5 dimer and the "distal" PDGFβR TMD [i.e., between E5(I) and PR(I) and between E5(III) and PR(II)]. The ability of each E5 dimer to simultaneously contact both PDGFβR molecules promotes dimerization of the receptor by contributing the dimerization energy of the E5 dimer to the energy of the complex. PDGFβR dimerization is promoted more strongly in the six-helix model, where two E5 dimers make this contribution, than in a four-helix model, where only a single E5 dimer contributes, providing another explanation for the presence of two E5 dimers in the complex. This arrangement also provides an explanation for the requirement for E5 dimerization. Finally, by occluding several faces of the PDGFβR TMDs, the bound E5 dimers also place constraints on possible orientations of the receptor TMDs relative to each other and confine the PDGFβR TMDs into a productive orientation that promotes signaling.

We can imagine three pathways for receptor dimerization. In the first pathway, the unstimulated PDGFβR exists in a monomer–dimer equilibrium, primarily in the monomeric form. The E5 dimer preferentially binds to the dimeric form of the PDGFβR TMDs and stabilizes it, forming a structure similar to the original four-helix model. This four-helix complex then recruits the second E5 dimer, which further stabilizes the interaction between the two PDGFβR TMDs, analogous to the in silico addition of a second E5 dimer to the four-helix complex to generate the six-helix complex. In the second pathway, an E5 dimer binds to a PDGFβR monomer. This three-helix complex then recruits a second PDGFβR TMD to generate the four-helix complex, which in turn recruits the second E5 dimer as described above. In the third pathway, two three-helix complexes dimerize to generate the final six-helix complex.

The proposed model of the PDGFβR TMDs within the six-helix model may also provide insight into the structure of the TMDs in receptors activated by ligand. In other receptor systems, the receptor TMDs may rotate relative to one another in adopting the active state in response to ligand binding (e.g., ref. 35). The asymmetric organization of the PDGFβR TMDs in the six-helix model may contribute to the asymmetric arrangement of the intracellular kinase domains in activated RTKs (36, 37). Because transphosphorylation is intrinsically asymmetric, the asymmetry in this model may help establish the most active form of the receptor signaling complex.

In summary, we have proposed and tested an atomically detailed six-helix model of the transmembrane complex of the BPV E5 oncoprotein and the TMD of the PDGFβR. Analysis of the complex isolated from mouse cells confirmed the central feature of the model, the presence of two E5 dimers in the complex. This model has a different subunit structure than previous models of the complex, which were based on experimental and modeling approaches that did not provide information about the stoichiometry or size of the complex. Thus, we have used computational modeling to derive the quaternary structure of a naturally occurring TMD complex, which was subsequently experimentally verified. The model proposed here provides an energetically plausible mechanism for the activation of the PDGFβR by this unique viral oncogene product and includes an asymmetry that may be important for maximal receptor activity. The structural features revealed in this analysis may also be used by other TMD complexes, including intramolecular TMD complexes that constitute the hydrophobic core of multipass transmembrane proteins, and the approach we describe should be applicable to gain chemical and structural insights into other transmembrane proteins of biological interest.

Materials and Methods

Detailed experimental methods are presented in *SI Materials and Methods*.

Rosetta Modeling. We used the ab initio module of Rosetta membrane protocol (Version 3.4) to generate a coarse-grained model of the complex consisting of two monomers of the BPV E5 protein and two TMDs of the PDGFβR. For the modeling, these protein segments were arranged in alternating order to reflect the antiparallel transmembrane orientation of the viral compared with the cellular protein. A series of criteria based on prior experimental evidence was then used to select a single model for detailed MD simulations. See *SI Materials and Methods* for details.

All-Atom MD Simulations. Amino acid side chains were added to the Rosetta model, which was then refined by all-atom MD simulations in a hydrated POPC lipid bilayer. MD simulations were performed by using the NAMD software (Version 2.9). Based on the results obtained with the four-helix model, similar MD simulations were carried out on complexes with alternative stoichiometry, including the six-helix complex consisting of two E5 dimers and two PDGFβR TMDs. See *SI Materials and Methods* for details.

Mapping PDGFβR Face Mutants. A series of full-length PDGFβR mutants containing alanine scanning substitutions in the TMD were constructed and expressed in IL-3–dependent BaF3 cells. After expression of the BPV E5 protein or the PDGF homolog, v-*sis*, IL-3 was removed, and growth factor independence was assessed. See *SI Materials and Methods* for details.

Coimmunoprecipitation Analysis. Differentially tagged E5 proteins were expressed in BaF3 cells either separately or together with full-length or truncated forms of the PDGFβR containing a wild-type TMD or a TMD containing a T513L mutation that blocks E5 binding. FLAG-tagged E5 protein was immunoprecipitated from detergent extracts with an anti-FLAG antibody, and associated E5 dimer containing the HA tag was detected by nonreducing SDS/PAGE and immunoblotting with anti-HA antibody. See *SI Materials and Methods* for details.

Blue-Native Gel Electrophoresis. BaF3 cells were established expressing the HA-tagged E5 protein and a truncated version of the PDGFβR consisting largely of the TMD of the receptor. Protein complexes were isolated and subjected to BN-PAGE under nondenaturing conditions. After electrophoresis, complexes containing the E5 protein or the truncated PDGFβR were detected by immunoblotting. A series of low-molecular-mass transmembrane protein size markers were electrophoresed on the same gel and detected by immunoblotting. See *SI Materials and Methods* for details.

Cloning, Tissue Culture, and Biochemical Analysis. Standard procedures were used for tissue culture, retrovirus production and transduction, in vitro mutagenesis, cloning, immunoprecipitation, and immunoblotting. See *SI Materials and Methods* for details.

Data Availability. Primary data that support the conclusions of this study are available from the corresponding authors upon request.

ACKNOWLEDGMENTS. We thank Michael Strickler (Yale University) for expert computational help and Nicholas Carriero (Yale University) for advice and guidance with the use of the Louise cluster at the Yale Center for Research Computing. We also thank Erin Heim for technical assistance, Christopher Petti for statistical analysis, and Jan Zulkeski for assistance preparing this manuscript. Computational modeling used the Extreme Science and Engineering Discovery Environment, supported by NSF Grant ACI-1053575 (to D.M.E.). This work was supported by NIH Grants CA037157 (to D.D.), GM073857 (to D.M.E.), and GM120642 (to F.N.B.).

1. DiMaio D, Petti LM (2013) The E5 proteins. *Virology* 445:99–114.
2. Burkhardt A, Willingham M, Gay C, Jeang K-T, Schlegel R (1989) The E5 oncoprotein of bovine papillomavirus is oriented asymmetrically in Golgi and plasma membranes. *Virology* 170:334–339.
3. Schlegel R, Wade-Glass M, Rabson MS, Yang Y-C (1986) The E5 transforming gene of bovine papillomavirus encodes a small, hydrophobic polypeptide. *Science* 233: 464–467.
4. Windisch D, et al. (2015) Hydrophobic mismatch drives the interaction of E5 with the transmembrane segment of PDGF receptor. *Biophys J* 109:737–749.
5. Windisch D, et al. (2010) Structural role of the conserved cysteines in the dimerization of the viral transmembrane oncoprotein E5. *Biophys J* 99:1764–1772.
6. Surti T, Klein O, Aschheim K, DiMaio D, Smith SO (1998) Structural models of the bovine papillomavirus E5 protein. *Proteins* 33:601–612.
7. Horwitz BH, Burkhardt AL, Schlegel R, DiMaio D (1988) 44-amino-acid E5 transforming protein of bovine papillomavirus requires a hydrophobic core and specific carboxyl-terminal amino acids. *Mol Cell Biol* 8:4071–4078.
8. Oates J, Hicks M, Dafforn TR, DiMaio D, Dixon AM (2008) In vitro dimerization of the bovine papillomavirus E5 protein transmembrane domain. *Biochemistry* 47: 8985–8992.
9. King G, Oates J, Patel D, van den Berg HA, Dixon AM (2011) Towards a structural understanding of the smallest known oncoprotein: Investigation of the bovine papillomavirus E5 protein using solution-state NMR. *Biochim Biophys Acta* 1808: 1493–1501.
10. Windisch D, Ziegler C, Bürck J, Ulrich AS (2014) Structural characterization of a C-terminally truncated E5 oncoprotein from papillomavirus in lipid bilayers. *Biol Chem* 395:1443–1452.
11. Mattoon D, Gupta K, Doyon J, Loll PJ, DiMaio D (2001) Identification of the transmembrane dimer interface of the bovine papillomavirus E5 protein. *Oncogene* 20: 3824–3834.
12. Adduci AJ, Schlegel R (1999) The transmembrane domain of the E5 oncoprotein contains functionally discrete helical faces. *J Biol Chem* 274:10249–10258.
13. Talbert-Slagle K, DiMaio D (2009) The bovine papillomavirus E5 protein and the PDGF β receptor: It takes two to tango. *Virology* 384:345–351.
14. Demoulin JB, Essaghir A (2014) PDGF receptor signaling networks in normal and cancer cells. *Cytokine Growth Factor Rev* 25:273–283.
15. Chen PH, Unger V, He X (2015) Structure of full-length human PDGFRβ bound to Its activating ligand PDGF-B as determined by negative-stain electron microscopy. *J Mol Biol* 427:3921–3934.
16. Goldstein DJ, Andresson T, Sparkowski JJ, Schlegel R (1992) The BPV-1 E5 protein, the 16 kDa membrane pore-forming protein and the PDGF receptor exist in a complex that is dependent on hydrophobic transmembrane interactions. *EMBO J* 11: 4851–4859.
17. Lai CC, Henningson C, DiMaio D (1998) Bovine papillomavirus E5 protein induces oligomerization and trans-phosphorylation of the platelet-derived growth factor beta receptor. *Proc Natl Acad Sci USA* 95:15241–15246.
18. Nappi VM, Schaefer JA, Petti LM (2002) Molecular examination of the transmembrane requirements of the platelet-derived growth factor beta receptor for a productive interaction with the bovine papillomavirus E5 oncoprotein. *J Biol Chem* 277:47149–47159.
19. Petti L, DiMaio D (1992) Stable association between the bovine papillomavirus E5 transforming protein and activated platelet-derived growth factor receptor in transformed mouse cells. *Proc Natl Acad Sci USA* 89:6736–6740.
20. Staebler A, et al. (1995) Mutational analysis of the beta-type platelet-derived growth factor receptor defines the site of interaction with the bovine papillomavirus type 1 E5 transforming protein. *J Virol* 69:6507–6517.
21. Meyer AN, Xu Y-F, Webster MK, Smith AE, Donoghue DJ (1994) Cellular transformation by a transmembrane peptide: Structural requirements for the bovine papillomavirus E5 oncoprotein. *Proc Natl Acad Sci USA* 91:4634–4638.
22. Edwards AP, Xie Y, Bowers L, DiMaio D (2013) Compensatory mutants of the bovine papillomavirus E5 protein and the platelet-derived growth factor β receptor reveal a complex direct transmembrane interaction. *J Virol* 87:10936–10945.
23. Klein O, et al. (1998) Role of glutamine 17 of the bovine papillomavirus E5 protein in platelet-derived growth factor beta receptor activation and cell transformation. *J Virol* 72:8921–8932.
24. Klein O, Kegler-Ebo D, Su J, Smith S, DiMaio D (1999) The bovine papillomavirus E5 protein requires a juxtamembrane negative charge for activation of the platelet-derived growth factor beta receptor and transformation of C127 cells. *J Virol* 73: 3264–3272.
25. Nilson LA, Gottlieb RL, Polack GW, DiMaio D (1995) Mutational analysis of the interaction between the bovine papillomavirus E5 transforming protein and the endogenous beta receptor for platelet-derived growth factor in mouse C127 cells. *J Virol* 69:5869–5874.
26. Drummond-Barbosa DA, Vaillancourt RR, Kazlauskas A, DiMaio D (1995) Ligand-independent activation of the platelet-derived growth factor beta receptor: Requirements for bovine papillomavirus E5-induced mitogenic signaling. *Mol Cell Biol* 15:2570–2581.
27. Petti L, DiMaio D (1994) Specific interaction between the bovine papillomavirus E5 transforming protein and the beta receptor for platelet-derived growth factor in stably transformed and acutely transfected cells. *J Virol* 68:3582–3592.
28. Goldstein DJ, et al. (1994) The bovine papillomavirus type 1 E5 transforming protein specifically binds and activates the beta-type receptor for the platelet-derived growth factor but not other related tyrosine kinase-containing receptors to induce cellular transformation. *J Virol* 68:4432–4441.
29. Muhle-Goll C, et al. (2012) Hydrophobic matching controls the tilt and stability of the dimeric platelet-derived growth factor receptor (PDGFR) β transmembrane segment. *J Biol Chem* 287:26178–26186.
30. Nappi VM, Petti LM (2002) Multiple transmembrane amino acid requirements suggest a highly specific interaction between the bovine papillomavirus E5 oncoprotein and the platelet-derived growth factor beta receptor. *J Virol* 76:7976–7986.
31. Petti LM, Reddy V, Smith SO, DiMaio D (1997) Identification of amino acids in the transmembrane and juxtamembrane domains of the platelet-derived growth factor receptor required for productive interaction with the bovine papillomavirus E5 protein. *J Virol* 71:7318–7327.
32. Yarov-Yarovoy V, Schonbrun J, Baker D (2006) Multipass membrane protein structure prediction using Rosetta. *Proteins* 62:1010–1025.
33. Reisinger V, Eichacker LA (2006) Analysis of membrane protein complexes by blue native PAGE. *Proteomics* 6:6–15.
34. Schägger H, von Jagow G (1991) Blue native electrophoresis for isolation of membrane protein complexes in enzymatically active form. *Anal Biochem* 199:223–231.
35. Seubert N, et al. (2003) Active and inactive orientations of the transmembrane and cytosolic domains of the erythropoietin receptor dimer. *Mol Cell* 12:1239–1250.
36. Mol CD, et al. (2003) Structure of a c-kit product complex reveals the basis for kinase transactivation. *J Biol Chem* 278:31461–31464.
37. Zhang X, Gureasko J, Shen K, Cole PA, Kuriyan J (2006) An allosteric mechanism for activation of the kinase domain of epidermal growth factor receptor. *Cell* 125: 1137–1149.
38. Kulke R, DiMaio D (1991) Biological properties of the deer papillomavirus E5 gene in mouse C127 cells: Growth transformation, induction of DNA synthesis, and activation of the platelet-derived growth factor receptor. *J Virol* 65:4943–4949.
39. Humphrey W, Dalke A, Schulten K (1996) VMD: Visual molecular dynamics. *J Mol Graph* 14:33–38, 27–28.
40. Wu EL, et al. (2014) CHARMM-GUI Membrane Builder toward realistic biological membrane simulations. *J Comput Chem* 35:1997–2004.
41. Phillips JC, et al. (2005) Scalable molecular dynamics with NAMD. *J Comput Chem* 26: 1781–1802.
42. Best RB, et al. (2012) Optimization of the additive CHARMM all-atom protein force field targeting improved sampling of the backbone φ, ψ and side-chain χ(1) and χ(2) dihedral angles. *J Chem Theory Comput* 8:3257–3273.
43. Klauda JB, et al. (2010) Update of the CHARMM all-atom additive force field for lipids: Validation on six lipid types. *J Phys Chem B* 114:7830–7843.
44. Jorgensen WL, Chandrasekhar J, Madura JD, Impey RW, Klein ML (1983) Comparison of simple potential functions for simulating liquid water. *J Chem Phys* 79:926–935.
45. Darden T, York D, Pedersen L (1993) Particle mesh eward—an N.log(N) method for ewald sums in large systems. *J Chem Phys* 98:10089–10092.
46. Essmann U, et al. (1995) A smooth particle mesh ewald method. *J Chem Phys* 103: 8577–8593.
47. Grubmuller H, Heller H, Windemuth A, Schulten K (1991) Generalized verlet algorithm for efficient molecular dynamics simulations with long-range interactions. *Mol Simul* 6: 121–142.
48. Feller SE, Yin D, Pastor RW, MacKerell AD, Jr (1997) Molecular dynamics simulation of unsaturated lipid bilayers at low hydration: Parameterization and comparison with diffraction studies. *Biophys J* 73:2269–2279.
49. Martyna GJ, Tobias DJ, Klein ML (1994) Constant pressure molecular dynamics algorithms. *J Chem Phys* 101:4177–4189.
50. Lam SS, et al. (2015) Directed evolution of APEX2 for electron microscopy and proximity labeling. *Nat Methods* 12:51–54.